ICCK Journal of Image Analysis and Processing
http://dx.doi.org/10.62762/JIAP.2025.421429

RESEARCH ARTICLE

Application and Deployment of a Fine-Tuned Pre-trained Deep Model for Breast Cancer Classification

Hmidi Alaeddine[1,2,*] **and Lina Tekari**[3]

[1] Higher Institute of Applied Sciences and Technology of Kasserine, University of Kairouan, Kasserine 1200, Tunisia
[2] Laboratory of Electronics and Microelectronics, Faculty of Sciences of Monastir, Monastir University, Monastir 5000, Tunisia
[3] Faculty of Medicine, Lucian Blaga University of Sibiu, Sibiu 550024, Romania

Abstract

Breast cancer remains one of the most significant health challenges, being the second leading cause of death among women worldwide. Early and accurate diagnosis is critical to improving treatment outcomes and increasing survival rates. In this study, we present an innovative application of the WRN-28-2 model, a deep convolutional neural network pre-trained on ImageNet, for the classification of histopathological breast cancer images from the BreakHis dataset. By leveraging transfer learning, the model was fine-tuned to differentiate between benign and malignant cases, achieving a remarkable classification accuracy of 99.16% on the test set. Moreover, the model outperformed existing state-of-the-art techniques on the same dataset. This research highlights the efficiency and adaptability of WRN-28-2 for medical image classification and opens avenues for its deployment in real-world diagnostic scenarios, particularly in resource-constrained environments.

Submitted: 31 August 2025
Accepted: 20 September 2025
Published: 08 November 2025

Vol. 1, **No.** 4, 2025.
10.62762/JIAP.2025.421429

***Corresponding author:**
✉ Hmidi Alaeddine
alaeddine.hmidi@issatkas.u-kairouan.tn

Keywords: wide ResNet, CNN, breakHis, classification, breast cancer, histopathological image.

1 Introduction

Breast cancer is one of the most frequently diagnosed diseases in women. It is a term for cells with extra mass growth in the breast area in women. The breast tissue forms this tumor which is classified as either benign or malignant. The malignant area is considered as the most affected cancerous area while the benign area is considered as the non-cancerous area.

According to breast cancer statistics, Chinese women are considered to have a 6.25% higher risk of being analyzed as breast cancer patients in their lifetime. Malaysian women have a 1 in 20 chance of being diagnosed with breast cancer in their lifetime [1]. Overall, statistics show that the incidence of breast cancer is around 12% of all cancer cases in the world. In addition, approximately 25% of women are diagnosed with breast cancer. Therefore, accurate and rapid analysis of breast cancer images is important for diagnosis.

Breast cancer survival rate is significantly affected by the stage of malignancy at diagnosis [2]. In this way, early identification is necessary to provide

Citation
Alaeddine, H., & Tekari, L. (2025). Application and Deployment of a Fine-Tuned Pre-trained Deep Model for Breast Cancer Classification. *ICCK Journal of Image Analysis and Processing*, 1(4), 162–171.

forensic treatment for breast cancer patients and to reduce depression and mortality [3] Early detection of mammograms based on computer-aided detection methods (CAD) may improve breast cancer treatment outcomes and extend survival time. Computer-assisted diagnosis approach is a widely used technique to classify breast cancer picture. It provides valuable information and uses general image classification techniques.

In the field of biomedicine, the examination and diagnosis of breast cancer histopathology by medical experts is a sensitive, expensive and time-consuming process. The examination and diagnosis process can be supported by leveraging technology development and using existing technology tools and programs. Thus, the diagnostic cost and effort can be greatly reduced. For this purpose, many studies and research have been carried out. In [15], support vector machines (SVM) equipped with a feature selection algorithm were used to detect breast cancer. This study obtained a success rate of 99.51%. SVM, Deep Neural Network (DNN) and other classifiers performed the classification. Generally, the feature selection process is done with bioinspired techniques. In [16], a system that combines association rules (RA) and neural network (NN) has been proposed for the diagnosis of breast cancer. Association rules ensured a reduction in the number of features while neural network was used for classification. The accuracy of the system was 95.6%.

Recently, many specialists have applied artificial neural networks (ANN) to different types of diseases [5]. The characteristic calculations of ANN have also been used to identify breast cancer disease [4]. We note that CNN has been applied to the classification of medical images in three main ways. The first method is to train the CNN from scratch [6–8]. The second method is to use a pre-trained CNN model to extract features from medical images [9–11] and the third method is to refine a pre-trained CNN model on medical data [12–14].

In [18], stromal (ST) and Epithelial (EP) that are two types of tissues in histological images have been segmented automatically using the deep convolutional neural network (DCNN). The model delivered interesting results. Images were classified using ImageNet's pre-trained DCNN model named AlexNet. As a result, model provides a superior accuracy with the deep fusion rules. A new breast cancer algorithm (CNNI-BCC) has been suggested in [17]. The CNNI-BCC model was proposed to support medical experts in diagnosing breast cancer in a timely manner. The CNNI-BCC model can classify incoming medical images as malignant, benign, or normal patients with sensitivity, accuracy, area under the receiver operating characteristic (AUC) curve, and specificity of 89.47%, 90.50%, 0.901 ±0.0314 and 90.71% respectively. In [22], a 152-layer learning-based residual convolutional neural network named ResHist for histopathological classification of breast cancer images is proposed. The proposed ResHist model achieves an accuracy of 84.34% and an F1 score of 90.49% for the classification of histopathological images. Also, the model achieves an accuracy of 92.52% and an F1 score of 93.45% when data augmentation is used. Dabber et al. [23] proposed an automatic breast cancer detection technique that gives a prediction accuracy of 99.86% for the actual class. They used CNN for feature extraction, and fully connected artificial neural network (ANN) for classification. In [24], Sagar showed how one can classify breast cancer from a collection of microscopic images using the DenseNet 201 model and transfer learning. It achieves an accuracy equivalent to 98.3%.

Kassani et al. [25] proposed an ensemble approach based on deep learning for Binary classification of breast histology images. The ensemble model combines three pre-trained CNNs: MobileNet, VGG19 and DenseNet. This ensemble model which adopts these three pre-trained CNNs is exploited for the entity representation and extraction stages. The extracted features are then fed into a multi-layer perceptron classifier to perform the classification task. The proposed method is tested on four datasets: PatchCamelyon, BreakHis, ICIAR and Bioimaging. The proposed ensemble method achieves accuracies of 98.13%, 95.00%, 94.64%, and 83.10% for BreakHis, ICIAR, PatchCamelyon, and Bioimaging datasets, respectively. Adeshina et al. [26] addressed the problem of intra-class classification of breast histopathology images into eight classes of benign or malignant cells. They adopted a DCNN architecture combined with the learning method. They achieved a cross-class classification accuracy of 91.5% with the BreakHis dataset. Han et al. [27] proposed a breast cancer multi-classification technique using a new deep learning model. The proposed model achieved an accuracy equivalent to 93.2%.

It can be seen that several models have been proposed to improve the accuracy of breast cancer diagnosis. It is well established that one of the favored models for the diagnosis of breast cancer is the deep learning approach [19–21, 23–28].

In the research that follows, we present our approach to the challenge with two objectives. The first objective is to study and determine the relevance of Wide ResNet(WRN) [30] for the task of classifying breast cancers. The second objective is to obtain the lowest possible error on a set of BreakHis test images. It should be noted that no study has attempted to address this aspect before, as this is the first work that addresses the field of breast cancer classification using WRN-28-2(WRN) [30]. The main contributions of this research are:

- We applied for the first time the WRN-28-2 [30] model on the BreakHis database for the classification of breast cancers.
- Presentation of an in-depth experimental study on the application of the WRN-28-2 model, particularly analyzing its effectiveness for classifying breast cancer from histopathological images in the BreakHis dataset.
- The use of data augmentation techniques significantly improved the model's performance, especially at a 200X magnification factor, resulting in increased accuracy and better generalization.
- The WRN-28-2 model was deployed on a low-cost embedded platform (Raspberry Pi), demonstrating the feasibility of using artificial intelligence in low-infrastructure medical environments, particularly in contexts sensitive to data privacy.
- A real-time inference solution was implemented, offering localized medical diagnosis without the need for an internet connection, which is especially relevant in mobile or remote healthcare environments.
- An extensive comparison of the WRN-28-2 model's performance, with and without data augmentation, and with existing models, highlighting its robustness and superiority for classifying breast cancer histopathological images.

These contributions emphasize the importance of the proposed approach in improving breast cancer diagnosis while ensuring the accessibility and effectiveness of solutions in diverse medical contexts.

This paper is organized as follows: Section 2 presents the Breast Cancer Histopathological Database (BreakHis) used for training the model and details the data augmentation techniques applied to enhance model performance. Section 3 discusses the methodology for applying the pre-trained WRN-28-2 model to histopathological image classification, focusing on the transfer learning approach. Section 4 outlines the experimental setup, including hardware and software configurations and training parameters. Section 5 presents the experimental results, comparing performance with and without data augmentation, and benchmarks the model against existing ones. This section also explores the model's performance on embedded platforms, particularly a Raspberry Pi, for low-cost, real-time classification. Section 6 discusses the study's limitations and future research directions for enhancing model robustness and expanding its application to other cancer types. Finally, Section 7 concludes the paper.

2 Dataset

In this section, we briefly describe the data set used in our work. Furthermore, this section details the proposed data augmentation technique.

2.1 Breast Cancer Histopathological Database (BreakHis)

The Breast Cancer Histopathology Database (BreakHis) [22] consists of 7909 microscopic RGB (Resolution: 700X460 pixels, 3 channels with 8-bit depth in each channel, PNG format) images of breast tumor tissue collected from 82 patients. BreakHis [22] is separated into two main groups: benign tumors and malignant tumors. It integrates 5,429 malignant samples and 2,480 benign samples. The images have 4 levels of magnification (40X, 100X, 200X and 400X). Figure 1 shows a malignant breast tumor slide seen in different magnifications: (a) 40X, (b) 100X, (c) 200X, and (d) 400X.

2.2 Data augmentation:

The performance of deep learning models is highly dependent on the size of the training data set available. In this work, we have proposed a data augmentation method, in which we use these three techniques: the image patch generation algorithm; affine transformation and stain normalization [29]. This data augmentation approach increases the size of the data set 4 times. Figure 2 presents an example of histopathological image data augmentation.

2.3 Dataset Split (Train/Test)

To ensure the validity of the results and avoid any data leakage, it is important to clarify the method

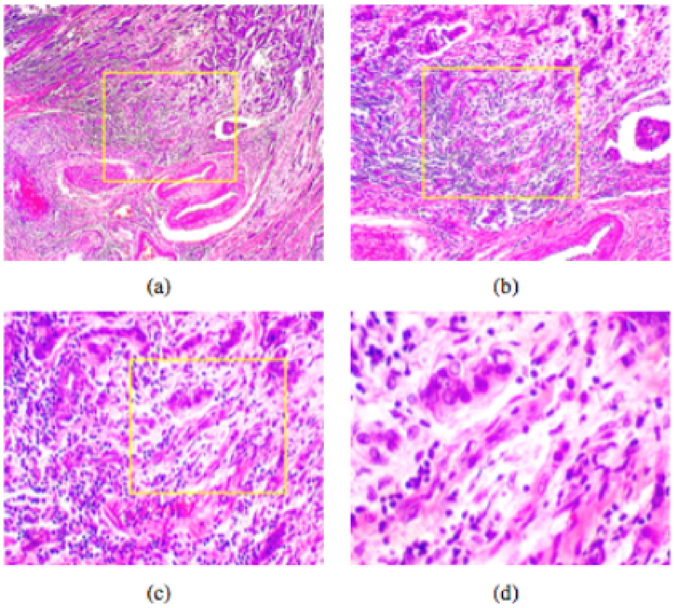

Figure 1. A slide of breast malignant tumor seen in different magnification factors: (a) 40X, (b) 100X, (c) 200X, and (d) 400X [22].

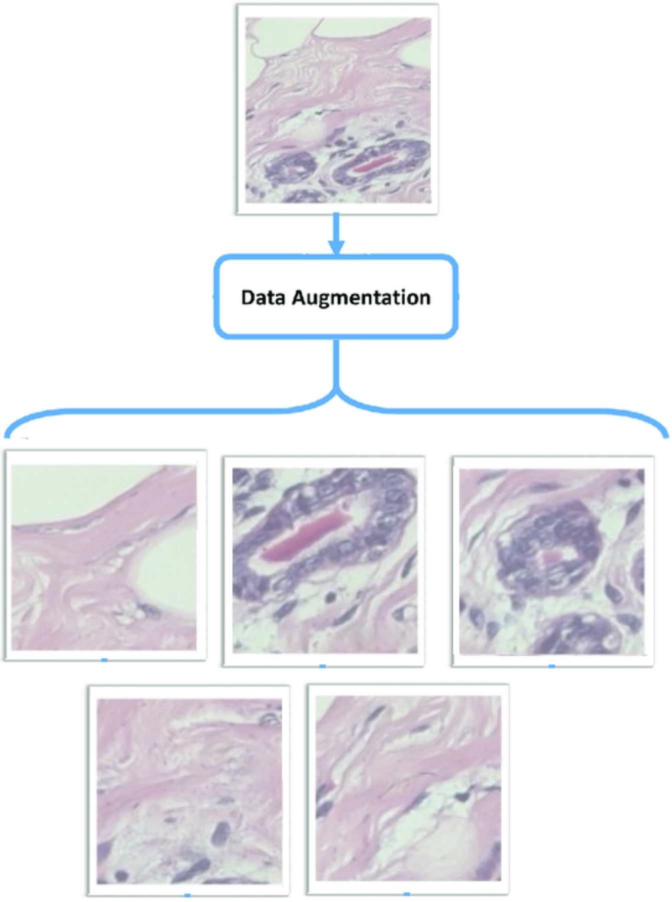

Figure 2. Example of histopathological image data augmentation [23].

used for splitting the dataset into training and test sets. In this study, we opted for an image-wise split, randomly allocating 70% of the images to the training set and 30% to the test set. It is important to note that images from the same patient do not appear in both sets. In other words, each patient contributes to only one of the two sets (training or test), ensuring complete independence between the training and test data.

The image-wise split ensures flexibility in using the dataset while providing a sufficiently large number of images for training. Additionally, by ensuring that no images from the same patient are present in both sets, we eliminate the risk of information leakage, which could skew the model evaluation, especially in a medical context where patient data can be similar or correlated.

This approach has the advantage of maximizing the diversity of images in both the training and test sets while maintaining the integrity of the evaluation. It is commonly preferred in medical image classification studies, where each image may contain patient-specific characteristics.

3 Methodology

In this work, we applied the WRN-28-2 [30] model in the field of classification of histopathological images of breast cancer. The proposed model uses the transfer learning technique of the powerful CNN WRN-28-2 [30] pretrained on ImageNet to train and classify the set "BreakHis" data in benign or malignant as well as the augmented BreakHis dataset. Figure 3 presents the schematic diagram of the proposed methodology.

Pretrained networks trained on the classified big dataset for different applications that can be used for the new application using transfer learning. In transfer learning, pre-trained network weights are used and adjusted according to the new application [23]. To fine-tune the network, the last layer (the softmax layer) of the network has been replaced with the new two-class softmax layer. Pre-trained networks require the input size to be the same as the input layer dimension. Therefore, the histopathological images in the database were resized to $224 \times 224 \times 3$ before applying them as input to the network.During fine-tuning, we have used 0.01 learning rate for newly added layers and 0.001 learning rate for the remaining layers.

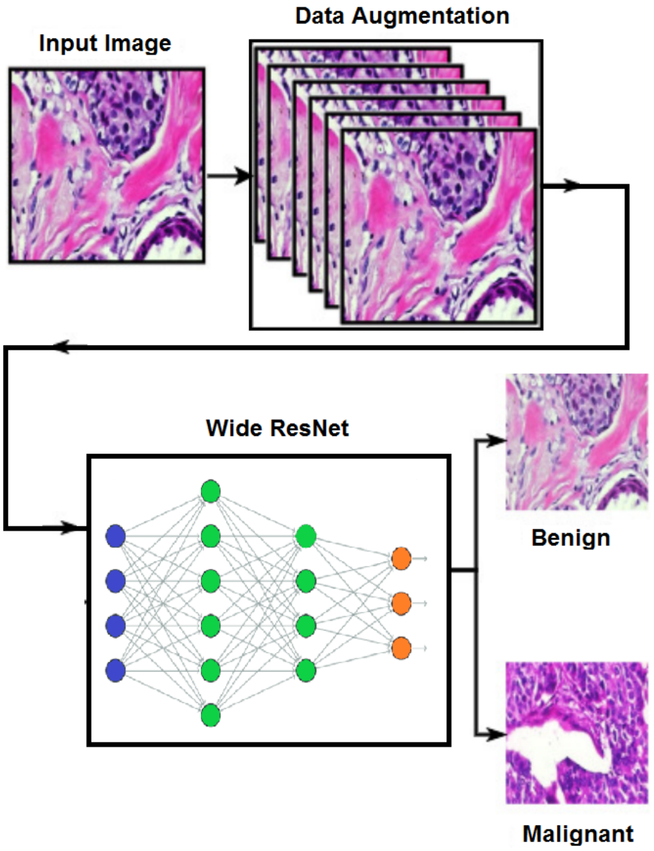

Figure 3. Block diagram of proposed method.

4 Experimental Setup

The WRN-28-2 [30] model was trained using the Adam optimizer, with differentiated learning rates: 0.01 for the newly added layers (softmax layer for binary classification) and 0.001 for the pre-trained layers from ImageNet. Fine-tuning was performed by replacing the original softmax layer with a new one tailored to the specific task of breast cancer classification, using transfer learning. The histopathological images were resized to 224 x 224 x 3 pixels before being used as input. The training was carried out in a Python 3.7 environment with TensorFlow 2.0, with the data randomly split into 70% for training and 30% for testing. An L2 regularization of 0.0001 was applied to prevent overfitting, and a batch size of 32 was chosen to optimize convergence while preserving memory resources. The model was trained for 100 epochs, with a random seed set to 42 to ensure reproducibility. The results were obtained from three separate trials, ensuring the robustness of the performance.

5 Experiments and Discussion

To accomplish this proposed classification task, we leveraged different development tools and packages, including the python 3.7 language as well as the tensorflow 2.0 package and other libraries. The data set was randomly split between the training set and the test set in a ratio of 70% and 30%. The results reported in this article are the average of three trials. All experiments were performed on a 2.50 GHz Dell Intel Core i7 and 16 GB RAM.

5.1 Evaluation Metrics

To assess the performance of the proposed work, we used precision, recall, F1 score and accuracy as evaluation measures. These measurements are calculated as indicated by the equations numbered 1 through 4. We notice that TP identifes the True Positive, TN identifies the True Negative, FP identifes the False Positive and FN identifes the False Negative.

$$Accuracy = \frac{TP + TN}{TP + TN + FP + FN}. \quad (1)$$

$$Sensitivity(Recall) = \frac{TP}{TP + FN} \quad (2)$$

$$Precision = \frac{TP}{TP + FP} \quad (3)$$

$$F1Score = \frac{2 \times (Recall \times Precision)}{Recall + Precision} \quad (4)$$

5.2 Experimental Results

In the following a presentation of the experimental results of the proposed approach evaluated on the original dataset and the dataset with augmentation. Two experiments were carried out for the training of the network. In the first experiment, we trained the WRN-28-2 model on the original BreakHis dataset. In the second set of experiments, we trained the WRN-28-2 model on the augmented BreakHis dataset. The results obtained are described in Table 1.

Table 1. Mean recognition accuracy (%) of the WRN model at different magnification factors.

Method	40X	100X	200X	400X
WRN	89.88	90.98	88.29	89.64
WRN+Aug	94.11	94.79	99.16	94.42

A significant performance improvement is noticed when data augmentation is used. The best accuracy of 99.16% was obtained for a magnification factor of 200X. On the other hand, in Table 2, we presented the evaluation of the WRN-28-2 model on the basis of evaluation measures described in the previous subsection. Thus, we observed that the WRN-28-2 model with increased data yields the best results for all magnification factors.

Table 2. Performance of WRN models at different widening factors.

Magnification	Method	Spec.	Recall	Precision	F1
40X	WRN	93.94	93.03	99.99	96.38
	WRN+Aug	92.61	94.63	99.20	96.86
100X	WRN	87.62	93.62	98.23	95.86
	WRN+Aug	89.95	96.18	98.51	97.33
200X	WRN	81.66	97.44	91.89	94.58
	WRN+Aug	92.26	99.33	99.87	99.60
400X	WRN	85.50	95.17	95.23	95.20
	WRN+Aug	88.26	95.55	97.47	96.50

5.3 Confusion Matrices and Performance Evaluation

In this section, we present the confusion matrices and associated performance metrics for the two experimental configurations of our **WRN** model: with and without data augmentation. The model was evaluated on a validation set consisting of 656 images, and the results are analyzed to compare the impact of data augmentation on the model's performance.

5.3.1 WRN without Data Augmentation

For the **WRN** configuration without data augmentation, the confusion matrix results are as follows:

Table 3. Confusion Matrix for WRN without data augmentation

	Benign	Malignant
Benign	TP = 447	FN = 11
Malignant	FP = 43	TN = 155

The results in Table 3 indicate that the model without data augmentation has a very good ability to identify positive examples (with a recall of 97.44%) and a decent precision for predicting benign cases (91.22%). However, the increase in false positives (FP = 43) remains a challenge, which is reflected in the relatively lower specificity (78.28%).

5.3.2 WRN with Data Augmentation

When data augmentation is applied to the **WRN** model, the confusion matrix shows a notable improvement in performance:

Table 4. Confusion Matrix for WRN with data augmentation

	Benign	Malignant
Benign	TP = 456	FN = 2
Malignant	FP = 1	TN = 136

As shown in Table 4, data augmentation significantly improves the model's performance, with an exceptional recall of 99.56% and nearly perfect precision of 99.78%. False positives (FP = 1) are also greatly reduced, resulting in a substantial increase in specificity (99.27%) and accuracy (99.16%). These results suggest that data augmentation helps the model generalize better, especially for predicting benign cases.

5.4 Performance Comparison

A comparison of the two configurations shows that data augmentation significantly improves the overall performance of the **WRN** model. Indeed, the augmented method achieves much higher precision and recall while substantially reducing false positives. In contrast, without augmentation, while the model maintains a good level of performance, it suffers from a higher number of false positives and lower specificity.

These results confirm the importance of data augmentation in classification tasks, especially for datasets where the classes are imbalanced or difficult to distinguish.

5.5 Comparison with Existing Models

The third table shows a comparison of the performance of the WRN model with other existing methods and models. Our method clearly outperformed the rest of the proposed work and methodologies mentioned in the Table 5.

Table 5. Accuracy comparison with state-of-the-art methods.

Ref	Method	Accuracy
[23]	Customized ResHist	84.34%
[24]	Customized LeNet-5 CNN	93.45%
[25]	Pre-Trained DenseNet201 CNN	98.30%
[26]	Pre-Trained Combined CNNs	98.13%
[27]	New Deep CNN (14 Layers)	91.50%
[28]	Deep CNN (CSDCNN)	93.20%
[30]	Pre-Trained ResNet-50 CNN	99.10%
Ours	Pre-Trained WRN-28-2 CNN	**99.16%**

6 Inference and Embedded Deployment: Raspberry Pi as a Low-Cost Edge Platform

6.1 Rationale for Embedded Deployment

To evaluate the feasibility of using our breast cancer classification model in real-world, low-infrastructure scenarios, we deployed the quantized WRN-28-2 model on a Raspberry Pi 4 Model B (1 GB RAM). This embedded deployment serves as a proof-of-concept for scenarios where internet connectivity, computational resources, and data privacy are critical concerns, such as rural clinics, mobile diagnostic units, or field-based educational setups. By running inference directly on a single-board computer (SBC), we eliminate the need for cloud-based processing, thereby improving patient data security and system autonomy. This approach aligns with growing interest in edge AI, where deep learning models are executed locally on compact, energy-efficient hardware.

6.2 Hardware and Software Configuration

All inference experiments were conducted using a Raspberry Pi 4, as illustrated in Figure 4 , equipped with a quad-core ARM Cortex-A72 processor (1.5 GHz) and 1 GB of LPDDR4 RAM. The device was configured with a 32 GB microSD card hosting the operating system and necessary software.

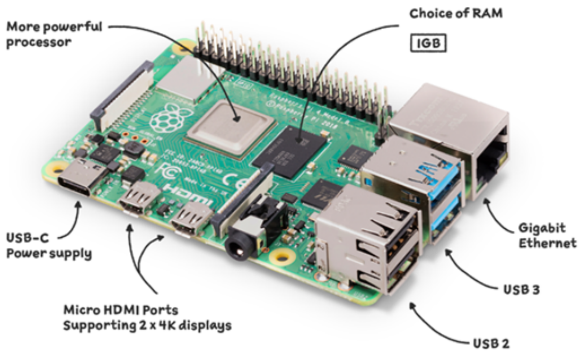

Figure 4. Raspberry Pi 4.

The WRN-28-2 model was optimized using post-training integer quantization and exported in `.tflite` format. This reduced both its memory footprint and computational cost, enabling deployment on constrained hardware without significant loss in classification performance.

6.3 Inference Pipeline on Raspberry Pi

The local inference pipeline was designed to be modular, efficient, and compatible with the Raspberry Pi's hardware limitations. It consists of the following stages:

1. **Image Capture:** The acquired images are stored on a USB drive, which is then connected to the Raspberry Pi. This process is straightforward, requires no network connection, and preserves data locally.
2. **Preprocessing:** Resizing to 224×224 pixels and normalization aligned with ImageNet statistics.
3. **Model Initialization:** Loading the optimized `.tflite` version of WRN-28-2.
4. **Inference Execution:** Running the model on the preprocessed image to generate a classification.
5. **Result Interpretation:** Applying a softmax threshold to determine class label (benign vs malignant).
6. **Output Display:** Displaying the prediction with probability score and optionally saving the result locally.

This setup enables offline, real-time decision-making while preserving patient data on-site.

6.4 Cross-Platform Performance Evaluation

To contextualize the Raspberry Pi's performance, we compared inference speed and memory usage with more powerful platforms. Table 6 summarizes the results across four hardware configurations.

Table 6. Average inference time per platform.

Platform	Avg. Inference Time (ms)
Raspberry Pi 4 (1 GB)	1065
Intel i5 CPU (6 GB RAM)	115
NVIDIA T4 GPU	42
NVIDIA A100 GPU	14

The Raspberry Pi achieved acceptable performance, completing inference in just over 1 second per image, suitable for low-throughput, high-security deployments. The CPU-based setup significantly reduced latency, while the T4 and A100 GPUs delivered sub-50 ms latency, highlighting their suitability for high-frequency or large-scale inference pipelines.

Although memory usage on the Raspberry Pi remained within acceptable bounds ($\sim$18 MB), it is important to note that quantization was key in enabling this level of efficiency. GPU memory usage was not included due to differences in memory management and optimization pipelines.

6.5 Discussion and Practical Implications

This comparative deployment study demonstrates the flexibility and scalability of the WRN-28-2 model:

- On embedded systems, such as the Raspberry Pi, it offers a practical solution for privacy-sensitive, low-resource environments where real-time cloud access is not possible.
- On cloud-oriented GPUs like the T4, the model supports real-time inference at scale, balancing cost and performance.
- On datacenter-grade GPUs such as the A100, it delivers ultra-low latency suitable for massive batch processing, real-time triage, or decision support systems in hospitals.

These results validate the edge-to-cloud adaptability of WRN-28-2 and suggest future directions in model pruning, quantization-aware training, or neural architecture search for even greater deployment efficiency.

6.6 Limitations and Future Work

While this study demonstrates the effectiveness of the WRN-28-2 model for breast cancer classification, several limitations should be acknowledged. **First**, the dataset used, although comprehensive, remains limited in size compared to the diversity of histopathological images encountered in clinical practice. A larger and more varied dataset could further improve the model's generalization and robustness. **Second**, the current work focuses exclusively on breast cancer, which restricts the applicability of the model to other types of cancer, such as lung or skin cancer. Expanding the methodology to multi-cancer classification would require additional annotated datasets and potential architectural adjustments.

Third, while the model achieves high accuracy, its deployment on resource-constrained devices, such as the Raspberry Pi, highlights the need for further optimization. Techniques like **quantization-aware training**, **model pruning**, or **neural architecture search** (**NAS**) could enhance inference speed and reduce memory usage without compromising performance. Additionally, the **interpretability** of deep learning models in medical diagnostics remains a challenge; integrating explainable AI (XAI) techniques could provide clinicians with clearer insights into the decision-making process.

Future work will address these limitations by:

- **Expanding the dataset** to include histopathological images from other cancer types, enabling multi-class classification.
- **Optimizing the model** for edge devices through advanced quantization and pruning, ensuring real-time performance in low-resource settings.
- **Exploring federated learning** approaches to improve model training while preserving patient data privacy.
- **Incorporating attention mechanisms** or transformers to capture more nuanced features in histopathological images.
- **Validating the model** in clinical trials to assess its reliability and usability in real-world diagnostic workflows.

These advancements will pave the way for broader applications of AI-driven diagnostic tools in oncology and beyond.

7 Conclusion

In this work, we explored the application of the pre-trained WRN-28-2 model for the automated classification of breast cancer from histopathological images. The model achieved an impressive classification accuracy of 99.16% on the BreakHis dataset with augmented data, demonstrating that our approach outperforms existing methods. More importantly, the model excels in its ability to classify whole slide images, preserving the global information of histopathological images while eliminating the need for data preprocessing.

Furthermore, a detailed analysis of the deployment across various hardware platforms, ranging from the Raspberry Pi as a low-cost embedded solution to datacenter GPUs such as the A100, validated the flexibility and efficiency of our model. The results highlight that the Raspberry Pi is a viable solution for scenarios requiring local autonomy and enhanced data privacy, particularly in resource-constrained environments.

Our work thus paves the way for broader applications of optimized deep learning models in various medical contexts. Future directions include performance improvements through advanced techniques, such as model pruning, quantization-aware training, and adaptation to other types of cancers and diseases. This research represents a significant step toward reliable, accessible, and deployable artificial intelligence solutions for medical diagnostics.

Although this study focuses on breast cancer, the proposed methodology could be extended to other types of cancer, such as lung or skin cancer, by adjusting the training techniques and using appropriate datasets.

Data Availability Statement

Data will be made available on request.

Funding

This work was supported without any funding.

Conflicts of Interest

The authors declare no conflicts of interest.

Ethical Approval and Consent to Participate

Not applicable.

References

[1] Youlden, D. R., Cramb, S. M., Dunn, N. A. M., Muller, J. M., Pyke, C. M., & Baade, P. D. (2012). The descriptive epidemiology of female breast cancer: An international comparison of screening, incidence, survival and mortality. *Cancer Epidemiology, 36*(3), 237–248. [CrossRef]

[2] Wang, L. (2017). Early Diagnosis of Breast Cancer. *Sensors, 17*(7), 1572. [CrossRef]

[3] Araújo, T., Aresta, G., Castro, E., Rouco, J., Aguiar, P., Eloy, C., ... & Campilho, A. (2017). Classification of breast cancer histology images using convolutional neural networks. *PloS one, 12*(6), e0177544. [CrossRef]

[4] Mohebian, M. R., Marateb, H. R., Mansourian, M., Mañanas, M. A., & Mokarian, F. (2017). A Hybrid Computer-aided-diagnosis System for Prediction of Breast Cancer Recurrence (HPBCR) Using Optimized Ensemble Learning. *Computational and Structural Biotechnology Journal, 15*, 75–85. [CrossRef]

[5] Wolterink, J. M., Leiner, T., Viergever, M. A., & Išgum, I. (2015, October). Automatic coronary calcium scoring in cardiac CT angiography using convolutional neural networks. In *International Conference on Medical Image Computing and Computer-Assisted Intervention* (pp. 589-596). Cham: Springer International Publishing. [CrossRef]

[6] Pan, Y., Huang, W., Lin, Z., Zhu, W., Zhou, J., Wong, J., & Ding, Z. (2015, August). Brain tumor grading based on neural networks and convolutional neural networks. In *2015 37th annual international conference of the IEEE engineering in medicine and biology society (EMBC)* (pp. 699-702). IEEE. [CrossRef]

[7] Shen, W., Zhou, M., Yang, F., Yang, C., & Tian, J. (2015, June). Multi-scale convolutional neural networks for lung nodule classification. In *International conference on information processing in medical imaging* (pp. 588-599). Cham: Springer International Publishing. [CrossRef]

[8] Van Ginneken, B., Setio, A. A., Jacobs, C., & Ciompi, F. (2015, April). Off-the-shelf convolutional neural network features for pulmonary nodule detection in computed tomography scans. In *2015 IEEE 12th International symposium on biomedical imaging (ISBI)* (pp. 286-289). IEEE. [CrossRef]

[9] Bar, Y., Diamant, I., Wolf, L., Lieberman, S., Konen, E., & Greenspan, H. (2015, April). Chest pathology detection using deep learning with non-medical training. In *2015 IEEE 12th international symposium on biomedical imaging (ISBI)* (pp. 294-297). IEEE. [CrossRef]

[10] Ciompi, F., de Hoop, B., van Riel, S. J., Chung, K., Scholten, E. T., Oudkerk, M., ... & van Ginneken, B. (2015). Automatic classification of pulmonary peri-fissural nodules in computed tomography using an ensemble of 2D views and a convolutional neural network out-of-the-box. *Medical image analysis, 26*(1), 195-202. [CrossRef]

[11] Schlegl, T., Ofner, J., & Langs, G. (2014, September). Unsupervised pre-training across image domains improves lung tissue classification. In *International MICCAI Workshop on Medical Computer Vision* (pp. 82-93). Cham: Springer International Publishing. [CrossRef]

[12] Carneiro, G., & Nascimento, J. C. (2013). Combining multiple dynamic models and deep learning architectures for tracking the left ventricle endocardium in ultrasound data. *IEEE transactions on pattern analysis and machine intelligence, 35*(11), 2592-2607. [CrossRef]

[13] Li, R., Zhang, W., Suk, H. I., Wang, L., Li, J., Shen, D., & Ji, S. (2014, September). Deep learning based imaging data completion for improved brain disease diagnosis. In *International conference on medical image computing and computer-assisted intervention* (pp. 305-312). Cham: Springer International Publishing. [CrossRef]

[14] Akay, M. F. (2009). Support vector machines combined with feature selection for breast cancer diagnosis. *Expert Systems with Applications, 36*(2), 3240–3247. [CrossRef]

[15] Karabatak, M., & Ince, M. C. (2009). An expert system for detection of breast cancer based on association rules and neural network. *Expert Systems with Applications, 36*(2), 3465–3469. [CrossRef]

[16] Spanhol, F. A., Oliveira, L. S., Petitjean, C., & Heutte, L. (2016). Breast cancer histopathological image

classification using Convolutional Neural Networks. In *2016 International Joint Conference on Neural Networks (IJCNN)* (pp. 2560–2567). [CrossRef]

[17] Ting, F. F., Tan, Y. J., & Sim, K. S. (2019). Convolutional neural network improvement for breast cancer classification. *Expert Systems with Applications, 120*, 103–115. [CrossRef]

[18] Xu, J., Luo, X., Wang, G., Gilmore, H., & Madabhushi, A. (2016). A deep convolutional neural network for segmenting and classifying epithelial and stromal regions in histopathological images. *Neurocomputing, 191*, 214-223. [CrossRef]

[19] Liao, Q., Ding, Y., Jiang, Z. L., Wang, X., Zhang, C., & Zhang, Q. (2019). Multi-task deep convolutional neural network for cancer diagnosis. *Neurocomputing, 348*, 66-73. [CrossRef]

[20] Khan, S., Islam, N., Jan, Z., Din, I. U., & Rodrigues, J. J. C. (2019). A novel deep learning based framework for the detection and classification of breast cancer using transfer learning. *Pattern Recognition Letters, 125*, 1-6. [CrossRef]

[21] Spanhol, F. A., Oliveira, L. S., Petitjean, C., & Heutte, L. (2016). A dataset for breast cancer histopathological image classification. *IEEE Transactions on Biomedical Engineering, 63*(7), 1455–1462. [CrossRef]

[22] Gour, M., Jain, S., & Kumar, T. S. (2020). Residual learning based CNN for breast cancer histopathological image classification. *International Journal of Imaging Systems and Technology, 30*(3), 621–635. [CrossRef]

[23] Dabeer, S., Khan, M. M., & Islam, S. (2019). Cancer diagnosis in histopathological image: CNN based approach. *Informatics in Medicine Unlocked, 16*, 100231. [CrossRef]

[24] Sagar, A. (2019). Convolutional Neural Network for Breast Cancer Classification: Deep Learning for solving the most commonly diagnosed cancer in women. *Towards Data Science, A Medium publication sharing concepts, ideas, and codes.*

[25] Kassani, S. H., Kassani, P. H., Wesolowski, M. J., Schneider, K. A., & Deters, R. (2019). Classification of histopathological biopsy images using ensemble of deep learning networks. In *Proceedings of the 29th Annual International Conference on Computer Science and Software Engineering* (pp. 92–99).

[26] Adeshina, S. A., Adedigba, A. P., Adeniyi, A. A., & Aibinu, A. M. (2018, November). Breast cancer histopathology image classification with deep convolutional neural networks. In *2018 14th international conference on electronics computer and computation* (*ICECCO*) (pp. 206-212). IEEE. [CrossRef]

[27] Han, Z., Wei, B., Zheng, Y., Yin, Y., Li, K., & Li, S. (2017). Breast cancer multi-classification from histopathological images with structured deep learning model. *Scientific Reports, 7*(1), 4172. [CrossRef]

[28] Magee, D., Treanor, D., Crellin, D., Shires, M., Smith, K., Mohee, K., & Quirke, P. (2009). Colour Normalisation in Digital Histopathology Images. In *Optical Tissue Image Analysis in Microscopy, Histopathology and Endoscopy: OPTIMHisE* (pp. 100-111). MICCAI.

[29] Zagoruyko, S., & Komodakis, N. (2016). Wide residual networks. In *Proceedings of the British Machine Vision Conference* (*BMVC*) (pp. 87.1–87.12). [CrossRef]

[30] Al-Haija, Q. A., & Adebanjo, A. (2020, September). Breast cancer diagnosis in histopathological images using ResNet-50 convolutional neural network. In *2020 IEEE International IOT, Electronics and Mechatronics Conference* (*IEMTRONICS*) (pp. 1-7). IEEE. [CrossRef]

Hmidi Alaeddine holds a Ph.D. in Electronics and Microelectronics and is currently an Assistant Professor at the University of Kairouan, Higher Institute of Applied Sciences and Technology of Kasserine, Tunisia. A former teacher at the Institute for the Blind in Sousse, his research focuses on the intersection of embedded electronics, IoT, FPGA, and artificial intelligence, particularly deep learning. His academic background is closely affiliated with the Laboratory of Electronics and Microelectronics (LR99ES30) at the University of Monastir. (Email: alaeddine.hmidi@issatkas.u-kairouan.tn)

Lina Tekari student at Lucian Blaga University of Sibiu, Faculty of Medicine, Bulevardul Victoriei 10, Sibiu 550024, Romania. (Email: linatekari1@gmail.com)